Loss of SORCS2 is associated with neuronal DNA double-strand breaks

Katerina O. Gospodinova[1], Ditte Olsen[2], Mathias Kaas[2], Susan M. Anderson[1], Jonathan Phillips[1], Rosie M. Walker[1,3], Mairead L. Bermingham[1], Abigail L. Payne[1], Panagiotis Giannopoulos[1], Divya Pandya[1], Tara L. Spires-Jones[4], Catherine M. Abbott[1], David J. Porteous[1], Simon Glerup[2], Kathryn L. Evans[1]

1. Centre for Genomic and Experimental Medicine, University of Edinburgh, Edinburgh, EH4 2XU, UK

2. Department of Biomedicine, Aarhus University, Aarhus, 8000, Denmark

3. Chancellor's Building, 49 University of Edinburgh, Edinburgh, EH16 4SB, UK (current address)

4. Centre for Discovery Brain Sciences, UK Dementia Research Institute, University of Edinburgh, Edinburgh, EH8 9XD, UK

Katerina O. Gospodinova: kgospodi@exseed.ed.ac.uk ; Ditte Olsen: olsen@biomed.au.dk; Mathias Kaas mko@biomed.au.dk; Susan M. Anderson S.M.Anderson@ed.ac.uk; Jonathan Phillips Jonathan.Phillips@ed.ac.uk; Rosie M. Walker: rwalke13@staffmail.ed.ac.uk; Mairead L. Bermingham: mairead.bermingham@ed.ac.uk; Abigail L. Payne: abbiepayne22@hotmail.com; Panagiotis Giannopoulos: s1582089@ed.ac.uk; Divya Pandya: divyapandya@hotmail.co.uk; Tara L. Spires-Jones: tara.spires-jones@ed.ac.uk; Catherine M. Abbott: c.abbott@ed.ac.uk; David J. Porteous: david.porteous@ed.ac.uk; Simon Glerup: glerup@biomed.au.dk; Kathryn L. Evans: Kathy.Evans@ed.ac.uk

Corresponding Author: Kathryn L. Evans, Centre for Genomic and Experimental Medicine, University of Edinburgh, Edinburgh, EH4 2XU, UK +44 131 651 8747

Abstract

SORCS2 is one of five proteins that constitute the Vps10p-domain receptor family. Members of this family play important roles in cellular processes linked to neuronal survival, differentiation and function. Genetic and functional studies implicate SORCS2 in cognitive function, as well as in neurodegenerative and psychiatric disorders. DNA damage and DNA repair deficits are linked to ageing and neurodegeneration, and transient neuronal DNA double-strand breaks (DSBs) also occur as a result of neuronal activity. Here, we report a novel role for SORCS2 in DSB formation. We show that SorCS2 loss is associated with elevated DSB levels in the mouse dentate gyrus and that knocking out *SORCS2* in a human neuronal cell line increased Topoisomerase IIβ-dependent DSB formation and reduced neuronal viability. Neuronal stimulation had no impact on levels of DNA breaks *in vitro*, suggesting that the observed differences may not be the result of aberrant neuronal activity in these cells. Our findings are consistent with studies linking the VPS10 receptors and DNA damage to neurodegenerative conditions.

Key words

SORCS2, DNA double-strand breaks, neuronal activity, neurodegeneration

Declarations

Funding

This work was supported by University of Edinburgh internal funds in the form of a PhD studentship, grants from Alzheimer's Research UK (ARUK-PPG2019B-015 and ARUK-NC2019-SCO) and by the UK Dementia Research Institute, which receives its funding from UK DRI Ltd funded by the UK Medical Research Council, Alzheimer's Society and Alzheimer's Research UK, and the European Research

Council (ERC) under the European Union's Horizon 2020 research and innovation programme (Grant agreement No. 681181).

Competing interests

Although not related to the present study, SG is a shareholder of Muna Therapeutics and Teitur Trophics, both involved in developing therapies directed at SorCS2. The remaining authors declare that they have no competing interests.

Availability of data and materials

Please contact author for data requests.

Code availability

Not applicable.

Authors' contributions

KOG and KLE conceived and planned the experiments. KOG performed the majority of the experiments and data analysis. SG provided the mice and DO and MK performed the behavioural experiments. SMA, JP, AP, PG and DP contributed to the execution of the experiments. RMW and MLB performed the statistical analysis of the mouse data. TSJ provided materials and support during assay optimisation. SG, CMA, TSJ and DJP contributed through strategic discussions. KOG and KLE wrote the manuscript with input from all authors.

Ethics approval

All experiments were approved by the Danish Animal Experiments Inspectorate under the Ministry of Justice (Permits 2011/561-119, 2016-15-0201-01127 and 2017-15-0201-01192) and carried out according to the ARRIVE guidelines.

Consent to participate

Not applicable.

Consent for publication

Not applicable.

88 **Introduction**

89 SORCS2 is a member of the VPS10p-domain receptor, or sortilin, family. The family comprises five
90 multifunctional neuronal receptors: sortilin; SORLA and SORCS1-3, which are characterised by
91 possession of a vacuolar protein sorting (VPS) 10p domain(Hermey 2009). All family members are
92 involved in intracellular sorting and trafficking of various neurotrophic factors, transmembrane
93 receptors and synaptic proteins, linking them to a broad range of cellular processes, including
94 neuronal function, differentiation and synaptic plasticity(Glerup et al 2014a).

95 Genetic and functional analyses implicate the VPS10p-domain receptors in cognitive functions and a
96 wide range of neurodegenerative and psychiatric disorders. Interrogation of the GWAS catalog
97 (https://www.ebi.ac.uk/gwas/) indicates that multiple SNPs in *SORCS2* are involved in epistatic
98 interactions that are associated ($p \leq 5x10^{-8}$) with paired helical filament tau (PHF-tau) levels (Wang et
99 al 2020).Genetic variants in *SORCS2* are also significantly associated ($p \leq 5x10^{-8}$) with alcohol
100 withdrawal (Smith et al 2018) and risk-taking behaviour (Karlsson Linnér et al 2019). In addition,
101 there are suggestive associations ($5x10^{-8} < p < 1x10^{-5}$) with ADHD (Alemany et al 2015), anorexia
102 nervosa (Duncan et al 2017), response to antidepressants (Fabbri et al 2018), depressive and manic
103 episodes in bipolar disorder (Fabbri and Serretti 2016), memory performance (Greenwood et al
104 2019), and intelligence (Davies et al 2018). Elevated *SORCS2* levels have been detected in the brains
105 of epileptic patients, as well as in the hippocampi of wild-type mice subjected to pentylenetetrazole
106 (PTZ)-induced kindling, a model of epilepsy (Malik et al 2019). Meanwhile, application of PTZ-
107 induced kindling in animals lacking *Sorcs2* increased the levels of oxidative stress and led to an
108 exacerbated oxidative stress response in primary neurons (Malik et al 2019). Increased *SORCS2*
109 expression has also been observed in response to application of the cortisol analogue,
110 dexamethasone (DEXA), as well as following alcohol exposure in a human neuroblastoma cell line
111 (Smith et al 2018). In mice, loss of *Sorcs2* has been linked to a decreased phenotypic preference for

112 alcohol and decreased alcohol withdrawal symptoms (Olsen et al 2019), suggesting a general role of
113 the receptor in the cellular and behavioural response to multiple stressors.

114 During mouse development (E15.5), *Sorcs2* is expressed in the ventral hippocampus and in tyrosine-
115 hydroxylase-positive (TH+) neurons of the midbrain. In the adult mouse brain, *Sorcs2* is strongly
116 expressed in hippocampal, striatal and cortical neurons (Deinhardt et al 2011; Glerup et al 2014b;
117 Glerup et al 2016). At the cellular level, in the hippocampus SorCS2 is located at the post-synaptic
118 density (PSD) of dendrites and within synaptic vesicles (Glerup et al 2016; Ma et al 2017). Through its
119 interactions with the BDNF receptor tyrosine kinase, TrkB, and the pro-BDNF receptor $p75^{NTR}$, it is
120 implicated in the induction of NMDA-dependent long-term potentiation (LTP) and depression (LTD)
121 in the hippocampus, respectively (Glerup et al 2016). Moreover, SorCS2 traffics TrkB to the PSD in an
122 activity-dependent manner, thus playing a role in synaptic tagging and synaptic potentiation
123 maintenance (Glerup et al 2016). The receptor has been also implicated in the trafficking of NMDA
124 receptor subunits to dendritic and synaptic surfaces in medium spiny neurons of the striatum (Ma et
125 al 2017) and in pyramidal neurons of the CA2 (Ma et al 2017; Yang et al 2020). In keeping with the
126 above findings, *Sorcs2*$^{-/-}$ mice exhibit learning and memory deficits (Glerup et al 2016) and
127 hyperactive behaviour on exposure to novelty (Olsen et al 2021).

128 DNA double-strand break (DSB) formation has been previously hypothesised to be involved in
129 learning and memory in wild-type mice via a behavioural task that involved exploration of a novel
130 environment (Suberbielle et al 2013; Madabhushi et al 2015). Suberbielle *et al.* (2013) (Suberbielle et
131 al 2013) reported the somewhat surprising finding of increased DSB formation in the hippocampus
132 and parietal cortex of adult wild-type mice following exploration of a novel environment. DSBs were
133 most abundant in the DG, an important area for learning and memory. The breaks were repaired
134 within 24 hours leading the authors to suggest that transient break formation plays a role in
135 chromatin remodelling and regulation of gene expression necessary for learning and memory
136 formation. Further experiments involving direct activation of the visual cortex and the striatum via

137 exposure to visual stimuli or optogenetic stimulation, respectively, showed that increases in
138 neuronal activity in the absence of the behavioural paradigm were sufficient for inducing DSBs.
139 Subsequent work by others showed that neuronal activity *in vivo* (induced via a contextual fear
140 conditioning training paradigm) and *in vitro* also resulted in higher levels of DSBs than was seen in
141 controls (Madabhushi et al 2015). Neuronal activity-induced DSBs were found to be located in the
142 promoters of a subset of early-response genes and mediated by the type II topoisomerase,
143 Topoisomerase IIβ (Topo IIβ): knockdown of Topo IIβ attenuated both DSB formation and early-
144 response gene expression following neuronal stimulation (Madabhushi et al 2015). In keeping with
145 these findings, *in vitro* pharmacological stimulation of neuronal activity has been shown to be
146 associated with increased DSB formation (Suberbielle et al 2013; Madabhushi et al 2015).

147 Given the changes in synaptic plasticity and the altered response to novelty and to stress observed in
148 the *Sorcs2*$^{-/-}$ mice, we hypothesised that loss of the receptor may lead to alterations in the number
149 of DNA DSBs at baseline, following exploration of a novel environment and/or following a recovery
150 period. In keeping with previous data, we detected an increase in DSB formation in the hippocampus
151 of wild-type mice following exploratory activity and repair of these breaks after a recovery period.
152 Compared to wild-type mice, *Sorcs2* knock-out mice had higher levels of DSBs in the DG at baseline
153 only. Next, we investigated whether this difference would also be observed in human neurons
154 lacking SORCS2. We used CRISPR/Cas9 genome editing to delete the gene from Lund Human
155 Mesencephalic (LUHMES) human neurons (Lotharius et al 2002; Scholz et al 2011). We found that
156 neurons from *SORCS2* knock-out lines had more DNA DSBs and were characterised by decreased
157 viability compared to wild-type lines. There was no difference in the number of breaks observed in
158 wild-type and knock-out lines following stimulation of neuronal activity.

159

160 **Materials and Methods**

161 Compounds and antibodies

162 Primary antibodies used in this study: polyclonal sheep anti-SORCS2 (AF4238, R&D Systems),
163 monoclonal mouse anti-γH2A.X (JBW301, Millipore) and polyclonal rabbit anti-53BP1 (NB100304,
164 Novus Biologicals). Secondary antibodies: rabbit anti-mouse Immunoglobulins/HRP (P0260, Dako),
165 rabbit anti-sheep Immunoglobulins/HRP (P0163, Dako), Alexa Fluor® 488 donkey anti-mouse IgG
166 (H+L) (A21202, Thermo Scientific) and Alexa Fluor® 568 donkey anti-rabbit IgG (H+L) (A21207,
167 Thermo Scientific). Etoposide was purchased from Sigma (E1383).

168 Animals

169 Mice were housed at the animal facility at Aarhus University, in groups of up to five mice per cage
170 with a 12-h light/12-h dark schedule and fed standard chow (1324, Altromin) and water *ad libitum*.
171 Cages were cleaned and supplied with bedding and nesting material every week. *Sorcs2*$^{-/-}$ mice had
172 been backcrossed for ten generations into C57BL/6J Bomtac background (Glerup et al 2014b). All
173 experiments were approved by the Danish Animal Experiments Inspectorate under the Ministry of
174 Justice (Permits 2011/561-119, 2016-15-0201-01127 and 2017-15-0201-01192) and carried out
175 according to the ARRIVE guidelines. Behavioural experiments were carried out using sex- and age-
176 matched mice (male, 5-6 months old). Each of the behavioural tests described below were carried
177 out using naïve animals in a randomized order by an investigator blinded to the mouse genotype. No
178 animals were excluded from the subsequent analysis.

179 Exploration of a novel environment

180 Mice in the control group (here defined as 'home cage') were kept in their original cages. Mice in the
181 novel environment ('novel environment') and the recovery from the novel environment ('recovery')
182 groups were transferred to the testing room, where they were individually exposed to a novel
183 environment. The novel environment consisted of an Open Field Arena with four different novel
184 objects and mint-like odour. Individual mice were allowed to explore the novel environment for 2h.
185 After the novel environment exploration, the mice in the novel environment group were sacrificed,
186 while the mice in the recovery group were returned to their home cages, where they recovered from

187 the behavioural task for 24h before being sacrificed. The mice from the home cage group were
188 sacrificed at the same time point.

189 Perfusion and tissue processing

190 Mice were perfused transcardially with cold PBS containing heparin (10,000 U/L), followed by ice-
191 cold 4% paraformaldehyde (PFA) in phosphate-buffered saline (PBS). Whole brains were dissected
192 and post-fixed overnight in 4% PFA in PBS. Following post-fixation, brains were rinsed in sterile PBS
193 and cryoprotected first in 10% sucrose and then in 30% sucrose at 4°C until the tissue sank to the
194 bottom of the tube. Brains were subsequently embedded in OCT compound on dry ice and stored at
195 -80°C. Coronal sections (14µm thick) containing the brain areas of interest (i.e., DG was sampled
196 from three regions: - 1.755mm, - 2.155mm and - 2.555mm relative to Bregma; CA2 and CA3 were
197 sampled from two regions: - 1.755mm and - 2.1550mm relative to Bregma) were obtained and
198 mounted on Superfrost slides. Slides were stored at −80°C.

199 LUHMES culture

200 LUHMES is a karyotypically normal human foetal mesencephalic cell line conditionally immortalised
201 with the v-myc oncogene. Proliferation of the neuronal precursor cells can be terminated by adding
202 tetracyclin, thus halting v-myc expression. Subsequent addition of GDNF results in robust
203 differentiation into post-mitotic dopaminergic neurons within five days. LUHMES cells (ATCC, RRID:
204 CVCL_B056) were grown and differentiated as described previously (Scholz et al 2011). Briefly, cell
205 culture dishes were pre-coated with PLO (1mg/ml; P3655, Sigma) and fibronectin (1mg/ml; F1141,
206 Sigma) in distilled H_2O (dH_2O) for at least 3h at 37°C. Following incubation, the coating solution was
207 aspirated, and plates/flasks were washed two times with dH_2O and completely air dried before cell
208 seeding. Prior to differentiation, LUHMES cells were maintained in proliferation medium consisting
209 of Advanced DMEM/F12 (12634028, Life Technologies), L-glutamine (200mM; 25030081, Life
210 Technologies), N2 supplement (100x; 17502-048, Life Technologies) and b-FGF (160µg/ml; 571502,
211 Biolegend). Experiments were conducted after 6 or 14 days of differentiation initiated by growing

212 cells in differentiation media consisting of Advanced DMEM/F12, L-glutamine (200mM), N2
213 supplement (100x), cAMP (100mM; D0627, Sigma), Tetracycline hydrochloride (1mg/ml; T7660,
214 Sigma) and recombinant human GDNF (20µg/ml; 212-GD-010, R&D). All experiments were initiated
215 with n=9 lines for each genotype, however, occasionally the neurons "lifted" from the
216 plastic/coverslip and that line was lost.

217 CRISPR/Cas9 Genome Editing

218 Guide RNAs (gRNAs) targeting *SORCS2* exon 1 or exon 3 were designed using two independent
219 online tools: the Zhang Lab CRISPR Design website (https://crispr.mit.edu) and CHOPCHOP
220 (https://chopchop.cbu.uib.no/), and were selected based on their on/off-target activity. The oligos
221 were phosphorylated and subsequently cloned into the px458 vector, co-expressing the Cas9
222 endonuclease and GFP (RRID: Addgene_48138). Low passage LUHMES cells were fed with fresh
223 proliferating media 2h prior to transfection. Cells were dissociated using TrypLE (12605036, Thermo
224 Scientific), counted and $2x10^6$ cells were transfected using the Basic Nucleofector kit for primary
225 neurons (VAPI-1003, Lonza) and the D-33 programme on the Amaxa Nucleofector II B device (Amaxa
226 Biosystems). 500µl of pre-warmed RPMI media (BE12-752F, Lonza) was added following
227 nucleofection. The cells were then incubated at 37°C for 5min and gently added to precoated 6-well
228 plates containing 2ml of freshly made proliferation medium. 2µg of the Cas9 plasmid containing the
229 gRNA of interest were used in each transfection. Empty vector (EV) control lines were generated by
230 transfecting proliferating LUHMES at an equivalent passage number with the px458 vector alone.

231 Forty-eight hours following transfection, cells were lifted as described before and centrifuged at 90g
232 for 10min. The cell pellets were resuspended in 500µl of warm PBS and GFP+ cells were sorted by
233 FACS into pre-coated 96-well plates, containing 100µl of freshly prepared proliferation medium.
234 After seven days, 100µl of fresh proliferation medium was added to each well, and three days later
235 single cell colonies were identified. At this stage, one third of the cells was kept for genotyping, and
236 the rest were split into two wells of a 24-well plate for further expansion.

237 CRISPR/Cas9 sgRNAs and Primer Sequences

238 gRNA *SORCS2* exon 1: CGGAGTGGCTTCGCGGGCGC

239 gRNA *SORCS2* exon 3: CCGTCATCGACAATTTCTAC

240 *SORCS2* exon 1 Forward primer: CCTTTCTCTGCGCTCTCG

241 *SORCS2* exon 1 Reverse primer: CCGCCCCTGATGACCATA

242 *SORCS2* exon 3 Forward primer: CAGAGTGCCCAGGACTGTAC

243 *SORCS2* exon 3 Reverse primer: ATGTGCCCTAGGTATGCAGG

244 Western blotting

245 Cells were lysed in ice cold 1% Triton lysis buffer (20mM Tris-HCl pH 8.0, 10mM EDTA, 1% Triton X-
246 100 and 1x protease inhibitor cocktail (5892970001, Roche)) and protein concentration was
247 measured using Bio-Rad BSA protein assay (5000116, Bio-Rad). Protein lysates were loaded on
248 NuPAGE Tris-acetate 3-8% precast gels (EA03752BOX, Life Technologies) and ran at 150V for 1.5h.
249 Gels were transferred onto PVDF membranes at 30V for 1.5h. Membranes were blocked in 5% milk
250 in 0.2% Tween-20 in TBS for 1h at room temperature and probed with primary antibodies against
251 SORCS2 (1:750; AF4238, R&D Systems) and GAPDH (1:10,000; MAB374, Merck) diluted in blocking
252 solution overnight at 4°C. After washes (3x 10min) in 0.2% Tween-20 in TBS, membranes were
253 incubated with secondary HRP-conjugated antibodies diluted 1:10,000 in blocking solution for 1h at
254 room temperature. After another three washes with TBS-0.2% Tween-20, blots were visualised using
255 the Pierce ECL Plus Western Blotting Substrate (11527271, Thermo Scientific) and exposed using
256 autoradiography film. Protein lysate obtained from HEK293 cells transfected with a plasmid
257 overexpressing a human *SORCS2* cDNA was used as a positive control.

258 Immunofluorescence staining

259 Slides containing brain sections were thawed at room temperature, incubated for 10min in 4% PFA
260 in PBS and then thoroughly washed for 30min in PBS containing 100mM glycine (1042011000, EMD
261 Millipore) followed by 30min in PBS. Heat-mediated antigen retrieval was performed by placing
262 slides in 1x sodium citrate buffer (PHR1416, Sigma), pH 6.0, and pulse-heated for 20min in the citrate
263 buffer in the microwave. Slides were allowed to cool for 20min inside the microwave, followed by
264 30min at room temperature. Slides were then washed 3 times (15min each wash) in PBS and
265 incubated in blocking solution for 1.5h at room temperature. Blocking solution contained 5% normal
266 donkey serum (D9663, Sigma), 1% BSA (421501J, VWR), 0.1% Triton-X and 0.05% Tween-20 in PBS.
267 Slices were incubated with monoclonal mouse anti-γH2A.X primary antibody (1:50; JBW301,
268 Millipore) in 5% normal donkey serum and 1% BSA in PBS at 4°C overnight. On the following day,
269 slides were further incubated for 30min at 37°C and washed 3 times in PBS (15min each wash).
270 Slides were then incubated with 3% Sudan black solution in 70% ethanol for 10min at room
271 temperature. After 3 rinses in dH_2O, slides were incubated with corresponding Alexa-conjugated
272 secondary antibody (1:500; A21202, Thermo Fisher) diluted in 5% normal donkey serum in PBS for
273 1h at 37°C. Slides were then washed 3 times in PBS, followed by 3 times in dH_2O (15min each wash).
274 DAPI (D9542, Sigma) diluted 1:1,000 in PBS was subsequently applied for 10min and washed off with
275 PBS (3 washes, 5min each). Sections were mounted in ProLong Gold antifade mountant (P36930,
276 Thermo Scientific).

277 Immunocytochemistry

278 Pre-differentiated (day 2) LUHMES were plated down ($0.15x10^6$ cells per well) and grown on acid-
279 etched coverslips, placed in 24-well plates and coated with PLO and fibronectin, followed by Geltrex
280 (A1413201, Thermo Scientific). Day 14 LUHMES neurons were fixed with 4% PFA for 15min, rinsed
281 with PBS and stored in TBS at 4°C until required. Neurons were permeabilised in 0.1% TBS-Triton X
282 for 5min. Following three rinses with TBS, coverslips were incubated in blocking solution (5% normal
283 donkey serum in 0.1% TBS- Tween) for 1h at room temperature and then overnight at 4°C with

284 primary antibodies diluted in blocking solution. The next day, neurons were washed with 0.1%
285 Tween-TBS (3x10min) and incubated with corresponding secondary antibodies for 1h at room
286 temperature. Secondary antibodies were diluted, together with DAPI (1:1,000; D9542, Sigma), in 4%
287 normal donkey serum in 0.1% TBS- Tween. Cells were washed with TBS (3x10min) and mounted with
288 ProLong Gold antifade mountant (P10144, Thermo Scientific). Primary antibodies used in this study
289 were: mouse monoclonal anti-γH2A.X (1:400; JBW301, Millipore), rabbit polyclonal anti-53BP1
290 (1:1000; NB100304, Novus Biologicals), mouse monoclonal anti-PSD93 (1:500; NBP2-58558, Novus
291 Biologicals), mouse monoclonal anti-synaptophysin (1:500; SMC-178D, StressMarq Bio.) and rabbit
292 monoclonal anti-GluR1 (1:500; 04-855, Millipore). Secondary antibodies were Alexa Fluor 488-
293 donkey anti-mouse IgG (1:300; A21202, Thermo Scientific), Alexa Fluor 596-donkey anti-rabbit IgG
294 (1:500; A21207, Thermo Scientific) and Alexa Fluor 647 Phalloidin (1:1000; A22287, Thermo
295 Scientific).

296 Treatments

297 For the etoposide treatment experiments, pre-differentiated (day 2) wild-type and *SORCS2* knock-
298 out LUHMES were plated down ($0.15x10^6$ cells per well) and differentiated until day 14. LUHMES
299 neurons were incubated with 0.5µM etoposide (E1383, Sigma) for 4h at 37°C prior to fixation. For
300 the experiments involving stimulation with glycine, pre-differentiated (day 2) wild-type and *SORCS2*
301 knock-out LUHMES were plated down ($0.05x10^6$ cells per well) and differentiated until day 14.
302 LUHMES neurons were incubated in a Mg^{2+} - free ACSF (125mM NaCl, 2.5mM KCl, 26.2mM $NaHCO_3$,
303 1mM NaH_2PO_4, 11mM glucose, and 2.5mM $CaCl_2$) supplemented with 300µM glycine (Sigma Aldrich)
304 for 5 min, followed by a 15 min incubation in ACSF containing 1.25mM $MgCl_2$ at 37°C prior to
305 fixation.

306 Image acquisition and analysis

307 All imaging and counting procedures were performed blind to genotype. Image analysis was
308 performed using the software package Fiji. Z-stacked confocal images, with a step size of 0.25µm

309 (brain sections) or 1µm (LUHMES neurons), were acquired on a Nikon STORM/A1+ microscope at
310 60x (brain sections) or 100x (LUHMES neurons) magnification, using the NIS Elements software. The
311 optimal laser intensity and gain that gave no signal in the no-primary antibody controls, were
312 established and kept constant for all subsequent analyses. Three images of each region of interest
313 were obtained from each mouse. The number of neurons with one or more γH2A.X-positive foci, as
314 well as the total number of nuclei within a given area (approximately 200 nuclei on average) were
315 counted manually and the percentage of γ-H2A.X-positive nuclei determined for each image. In the
316 case of LUHMES neurons, nine independent wild-type and nine independent *SORCS2* knock-out lines
317 were analysed. Approximately 100 nuclei (from four images belonging to different regions of the
318 same coverslip) were counted for each line, and the number of γH2A.X/53BP1-positive foci per
319 nucleus was calculated.

320 Quantitative reverse transcriptase PCR (qRT-PCR)

321 Cell pellets from day 14 LUHMES neurons were resuspended in RLT buffer (Qiagen) with 10% (v/v) 2-
322 mercaptoethanol. Total RNA was extracted using the RNeasy mini kit (Qiagen), and 1µg per sample
323 was reverse transcribed with Multiscribe Reverse Transcriptase using random hexamers in a 80µl
324 reaction. Controls, in which 25ng RNA of each sample was used to make cDNA in the absence of the
325 Multiscribe Reverse Transcriptase, were included to detect genomic contamination.

326 PCR amplification of the cDNA obtained for each sample was quantified using the TaqMan®
327 Universal PCR Mix No AmpErase® UNG (Life Technologies), and the threshold cycle (Ct) was
328 determined using the Applied Biosystems 7900HT Fast Real-Time PCR System and the corresponding
329 SDS software. TaqMan probes were used for the detection of *TOP2B* and eight reference genes
330 (*CYC1*, *ERCC6*, *SDHA*, *TOP1*, *RPLPO*, *SCLY*, *TBP* and *UBE4A*). The GeNorm software was used to
331 identify the most stably expressed reference genes (*SDHA* and *UBE4A*). A standard curve, generated
332 from a dilution series, was run for *TOP2B* and the reference genes. The baseline and Ct values were
333 determined for each gene and expression levels were calculated using the standard curve method

334 for absolute quantification, where unknowns are compared to the generated standard curve and
335 values are extrapolated. *TOP2B* expression values were subsequently normalised to the geometric
336 mean of the reference genes.

337 Viability assay

338 Neuronal viability was assessed using the Alamar Blue assay (DAL1025, Thermo Scientific). This assay
339 was chosen as: 1) it does not interfere with cell functioning and 2) it is not an end-point assay, i.e. it
340 allows viability to be measured at multiple time points (Rampersad 2012). Viability was measured at
341 day 6 and day 14 from an equivalent number of neurons ($0.25x10^6$) per line by replacing the medium
342 with freshly made differentiation medium containing 10% (v/v) Alamar Blue solution. Cells were
343 incubated with the Alamar Blue solution for 2h, after which the solution was transferred to a new
344 24-well plate and fluorescence measured in a FLUOstar OMEGA plate reader using an excitation
345 wavelength of 540-570nm, and an emission wavelength of 580-610nm.

346 Statistical analysis

347 Normal distribution and variance homogeneity were assessed for each dataset (Suppl. Table 1) using
348 the Shapiro-Wilk normality and an F test, respectively. Where linear regression models were used,
349 normal distribution and variance homogeneity of the residuals were assessed using the Shapiro-Wilk
350 normality test and the Spearman's rank correlation test for heteroscedasticity, respectively. When
351 the assumptions of normal distribution and homogeneity of variance were met, parametric tests
352 were performed, and the data was expressed as mean ± SD. Otherwise, the data was reported as
353 median with interquartile range and analysed using non-parametric tests. Differences between two
354 means were assessed using unpaired Student's t-test (two-tailed; for parametric data) or Mann
355 Whitney test (two-tailed; for non-parametric data). Two-way ANOVA was performed when multiple
356 means were compared. Statistical analyses were performed using GraphPad Prism. Sample sizes
357 were estimated based on previously reported findings (Suberbielle et al 2013) or pilot experiments
358 and calculated using the G-power software. Null hypotheses were rejected when $p<0.05$. Inclusion

359 criteria were: number of animals available for the mice; number of cell lines available following
360 genome editing and production of neurons. There were no exclusion criteria. Outlier removal was
361 not performed.

362

363 **Results**

364 Our goals were to investigate whether exploration of a novel environment led to a temporary
365 increase in the number of DSBs detected in the mouse brain in our hands and ii) whether deletion of
366 *Sorcs2* in mice leads to higher levels of DSB formation upon exploration of a novel environment
367 and/or a deficit in break repair. The novel environment paradigm comprised three groups of mice (5-
368 6 months of age): those that a) remained in their home cage (baseline group); b) explored a novel
369 environment (novel environment group) and c) explored a novel environment, followed by a
370 recovery period in the home cage (recovery group), before they were sacrificed (Fig. 1a). As
371 described previously (Suberbielle et al 2013), the proportion of neurons positive for γH2A.X (a widely
372 used marker of DNA DSBs in neurons and other cell types) was determined in three brain regions
373 (DG, CA2 and CA3 of the hippocampus, Suppl. Fig. 2; Suppl. Table 2).

374 In wild-type mice in each of the three brain regions, we observed a similar pattern to that described
375 by Suberbielle et al. (2013), i.e. wild-type mice exposed to the NE had more cells with DSBs than the
376 mice in the baseline and the recovery groups (Fig. 1b, left). In contrast, this pattern was not present
377 in the *Sorcs2*$^{-/-}$ mice, which, to our surprise, appeared to have a greater percentage of DSB-positive
378 nuclei at baseline (Fig. 1b, right). Given these results, we next sought to test the finding of a higher
379 number of breaks at baseline in the DG of the *Sorcs2*$^{-/-}$ mice using an independent set of age and sex-
380 matched wild-type and knock-out $^{-}$ mice. We detected significantly higher levels of DSBs in the
381 *Sorcs2*$^{-/-}$ mice ($U = 4$, $p = 0.03$; Fig. 1c).

382 Having determined that the *Sorcs2*$^{-/-}$ mice had higher levels of DNA DSBs at baseline we set out to
383 investigate whether this phenotype was also present in human neurons lacking *SORCS2*. We used
384 CRISPR/Cas9 genome editing (Fig. 2a) to delete the gene in the human neuronal cell line, LUHMES, a
385 karyotypically normal foetal mesencephalic cell line that can be robustly differentiated into post-
386 mitotic dopaminergic neurons (Suppl. Fig. 3), with the majority of cells generating trains of
387 spontaneous action potentials after 10-12 days of differentiation (Scholz et al 2011). Loss of *SORCS2*
388 expression was shown by western blotting (Fig. 2b; Suppl. Fig. 4). Nine independent lines were
389 generated using two different gRNAs (four produced using a gRNA targeting exon 1 and five from the
390 exon 3 gRNA) were used in all subsequent analyses.

391 To evaluate the effect of knocking out *SORCS2* on DNA DSB formation in human neurons, we stained
392 untreated control (consisting of wild-type (WT) and empty vector (EV) lines) and *SORCS2* knock-out
393 LUHMES neurons (day 14) for γH2A.X and 53BP1. The latter protein is quickly recruited to DSB sites,
394 where it binds to γH2A.X and acts as a scaffold for the binding of additional DNA repair proteins from
395 the non-homologous end joining (NHEJ) pathway, the main DNA repair pathway in post-mitotic cells
396 (Firsanov et al 2011). As previously reported for neurons (Crowe et al 2006), more than 90% of the
397 analysed neurons (wild-type and knock-out) had fewer than three double positive foci per nucleus,
398 with the majority of nuclei having no foci (Figure 3A; top row). There was no significant difference in
399 the number of foci per nucleus between control and *SORCS2* knock-out neurons ($U = 29$, $p = 0.34$;
400 Fig. 3b). Comparable levels of DSBs were observed between the WT and EV lines (Suppl. Fig. 5a), as
401 well as between the *SORCS2* KOs generated by targeting exon 1 and exon 3 ($U = 7$, $p = 0.556$, Suppl.
402 Fig. 5b). As DNA DSBs are rare, due to their dynamic repair, we next assessed whether *SORCS2* loss
403 would have an effect on the number of DSBs following treatment with etoposide, which causes
404 accumulation of Topoisomerase II (TopoII)-dependent DNA DSBs, by preventing their re-ligation
405 through stabilisation of the TopoII-DNA cleavable complex (Montecucco et al 2015). As expected,
406 etoposide treatment greatly increased the number of DSBs per nucleus in both wild-type and
407 *SORCS2* knock-out LUHMES neurons Fig. 3a). However, comparing the number of γH2A.X/53BP1-

408 positive foci per nucleus between etoposide-treated wild-type and *SORCS2* knock-out lines showed a
409 significant increase in the SORCS2$^{-/-}$ lines (t_2 = 2.148, p = 0.047;Fig. 3c). There was no significant
410 difference in the number of γH2A.X/53BP1-positive foci per nucleus between the *SORCS2* knock-out
411 clones derived by targeting exon 1 and those generated by disrupting exon 3 (U = 9, p = 0.905; Fig.
412 3d). No difference was observed between the two control groups, either, Suppl. Fig. 5c).

413 Topoisomerase IIβ (TopoIIβ) is the active form of topoisomerase in terminally differentiated cells,
414 such as neurons. Treatment with etoposide had no impact on expression levels of *TOP2B*, which
415 encodes TopoIIβ ($F_{1,\ 16}$ = 0.978, p = 0.337, Suppl. Fig. 6). In addition, there was no significant
416 difference in *TOP2B* levels between genotypes either prior to or following etoposide treatment ($F_{1,\ 16}$
417 = 2.652, p = 0.123, Suppl. Fig. 6).

418 Given the link between neuronal activity and TopoIIβ-mediated DNA DSBs (Madabhushi et al 2015),
419 we next investigated whether an established paradigm of neuronal stimulation would have a
420 differential impact on the formation of DNA DSBs in *SORCS2* knock-out and wild-type LUHMES
421 neurons. Incubation with glycine (300µM) led to an increase in the number of DNA breaks (Fig. 7a
422 and b). Treatment with glycine was also associated with a significant reduction in the somatic
423 surface area occupied by AMPA receptors, indicative of stimulation of neuronal activity (t_7 = 2.606, p
424 = 0.035, Suppl. Fig. 7c and d). We next compared the impact of glycine treatment in control (WT and
425 EV) and *SORCS2*$^{-/-}$ lines. No significant difference in the number of DNA DSB foci was observed
426 between the two groups (t_{14} = 0.383, p = 0.708, Fig. 4).

427 Finally, given the potential negative impact of DSB formation on neuronal function and survival, we
428 examined the effect of knocking out *SORCS2* on the overall neuronal viability both at early (day 6)
429 and late (day 14) stages of differentiation. At day 6, there was no significant difference in the
430 viability of wild-type neurons compared to that of the *SORCS2* knock-out clones (t_{16} = 0.296, p =
431 0.771; Fig. 5a). However, at day 14, we detected a significant reduction in the viability of *SORCS2*$^{-/-}$
432 clones compared to controls (t_{15} = 3.387, p = 0.004; Fig. 5b).

433 **Discussion**

434 Our data in wild-type mice are in agreement with the results of Suberbielle et al (2013), who showed
435 that exploration of a novel environment is associated with the acquisition of DNA DSBs, which are
436 repaired after a recovery period. We found, however, no evidence to support our initial hypothesis
437 that *Sorcs2* knock-out mice would show a greater number of breaks associated with the exploratory
438 behaviour or impaired recovery from this experience. In contrast, somewhat surprisingly, we
439 observed higher levels of DNA DSBs in the DG of *Sorcs2*$^{-/-}$ mice that remained in their home cage. We
440 subsequently confirmed this in an independent set of knock-out and wild-type mice.

441 We next investigated whether higher levels of DNA DSBs would be also found in human neurons
442 lacking *SORCS2*. DNA DSBs were rare in both mutant and wild-type lines, as has been reported
443 previously for rat primary cortical neurons (Crowe et al 2006), and there was no detectable
444 difference in γH2A.X immunoreactivity between the genotypes. As expected, treatment with the
445 TopoIIβ inhibitor, etoposide, led to an increase in the number of breaks in both lines. The *SORCS2*$^{-/-}$
446 lines, however, had significantly more breaks following etoposide treatment. Despite the increased
447 number of TopoIIβ-dependent breaks in the knock-out cell lines, there was no difference in *TOP2B*
448 expression levels in mutant lines either before or after treatment with etoposide. As enhanced
449 TopoIIβ activity and DSB levels have been observed following stimulation of neuronal activity
450 (Madabhushi et al 2015), we next investigated whether stimulation of neuronal activity would lead
451 to a differential response in the neurons lacking SORCS2. We found no evidence that loss of SORCS2
452 rendered the human neurons more susceptible to neuronal activity-evoked DNA DSBs. This result is
453 in keeping with our finding that *Sorcs2*$^{-/-}$ mice appeared to have a similar number of DNA DSBs to
454 wild-type mice following exploration of a novel environment; however, further work is required to
455 determine both the impact of neuronal activation in mice and in other types of human neurons.

456 There are a number of potential explanations for the link between SORCS2 loss and DNA DSBs.
457 Previous work (Malik et al 2019) implicated SorCS2 in protection against the oxidative stress-induced

458 DNA damage and neuronal loss caused by a PTZ-induced kindling paradigm. Similarly, Smith *et al.*
459 (2018) showed that *SORCS2* expression is stimulated by other stressors, such as alcohol and DEXA
460 (Smith et al 2018). DEXA administration induces DNA damage, which can be prevented by
461 application of reactive oxygen species (ROS) blockers (Ortega-Martínez 2015), thus SORCS2 loss may
462 exacerbate the effect of cellular stressors on DNA damage. Previous work (Morotomi-Yano et al
463 2018) provides evidence for the participation of Topo IIβ in the cellular response to DSBs induced by
464 laser microirradiation. It is possible, therefore, that etoposide treatment brings to light
465 topoisomerase-mediated repair of breaks caused by loss of SORCS2, but independently of
466 topoisomerase activity. Future experiments could test this hypothesis. Another possibility is that
467 SORCS2 loss impacts the number of DNA DSBs through loss of interaction with DNA repair proteins.
468 SORCS2 has been shown to co-localise with the transactivation response DNA-binding protein of
469 43kDa (TDP-43) in ALS post-mortem brains (Miki et al 2018). TDP-43 is an RNA/DNA-binding protein
470 that has recently been implicated in DSB repair (Mitra et al 2019). SORCS2 also interacts with
471 Heterogeneous Nuclear Ribonucleoprotein U (hnRNP-U) (Fasci et al 2018). This DNA and RNA
472 binding protein interacts with NEIL1, a DNA glycosylase implicated in the repair of DNA damaged by
473 reactive oxygen species, stimulating its base excision activity (Hegde et al 2012). Given the role of
474 the VPS10P family in intracellular trafficking, future work could investigate whether SORCS2 is
475 involved in trafficking the above proteins.

476 While the cellular mechanism underlying the increase in DNA DSBs associated with SORCS2 loss is
477 still uncertain, it is of interest that mature (but not immature) *SORCS2*$^{-/-}$ neurons showed decreased
478 viability, in keeping with findings in mouse primary neurons lacking Sorcs2, which show higher rates
479 of apoptosis (independent of autophagy) when subject to lysosomal stressors (Almeida at al.,
480 submitted). The maintenance of genome integrity is very important, particularly for post-mitotic
481 long-lived cells, such as neurons, and DNA damage is linked to neurodegenerative disorders, ageing
482 and decreased expression of genes important for brain maintenance and function (Madabhushi et al

483 2015). Further work is required, however, to investigate which aspect(s) of SORCS2 function underlie
484 the observed decrease in viability.

485 This study is subject to a number of limitations. An important factor is the small number of replicates
486 performed for the animal-based experiments, in particular. It is notable however that the set up was
487 sufficient to reproduce the pattern seen by Suberbielle et al. in wild-type mice undergoing the novel
488 environment task (Suberbielle et al 2013) and that we replicated the finding of increased numbers of
489 breaks in the mutant mice that remained in the home cage in an independent set of mice. It is also
490 notable that experiments performed in mice and a human cell line lacking SORCS2 both showed that
491 SORCS2 loss was associated with a greater number of DNA DSBs. Further work is required to
492 determine whether there are common or unique mechanisms underlying the findings.

493 In summary, we have shown that SorCS2 loss in mice leads to higher levels of γH2A.X-positive DNA
494 breaks. Loss of SORCS2 in human neurons led to an increase in the number of TopoIIβ-dependent
495 breaks and decreased neuronal viability. Our findings in both species suggest that the impact of
496 SORCS2 loss is not mediated by a differing response to neuronal activation. An increase in DNA DSBs
497 may lead to an altered transcriptional profile, affect genome integrity and ultimately lead to cell
498 death. In agreement with this notion, DNA damage is increasingly being linked to cognitive
499 impairment, dementia and other neurodegenerative disorders (Mullaart et al 1990; Adamec et al
500 1999; Madabhushi et al 2014; Shanbhag et al 2019; Thadathil et al 2019), and attenuating the DNA
501 damage response to DSBs has been demonstrated to be protective in models of several
502 neurodegenerative disorders (Tuxworth et al 2019). Our findings are in keeping with the known
503 involvement of other sortilin family members in cognition, ageing and neurodegenerative disorders
504 and with the recent finding that SNPs in *SORCS2* are involved in epistatic interactions associated with
505 pathological hallmarks of Alzheimer's disease (Wang et al 2020). Future experimental work should
506 assess hypotheses based around SORCS2's role in the cellular response to stress and/or DNA repair

507 pathways and measure the impact of loss of Sorcs2 on the epigenome and transcriptome of the
508 ageing dentate gyrus.

509

510 **Abbreviations**

511 **53BP1:** p53-binding protein 1

512 **ADHD:** Attention deficit hyperactivity disorder

513 **ALS:** Amyotrophic lateral sclerosis

514 **BDNF:** Brain-derived neurotrophic factor

515 **BSA:** Bovine serum albumin

516 **Ct:** Cycle threshold

517 **DEXA:** Dexamethasone

518 **DG:** Dentate gyrus

519 **DSB:** Double-strand break

520 **EV:** Empty vector

521 **FACS:** Fluorescence-activated cell sorting

522 **GDNF:** Glial cell-derived neurotrophic factor

523 **gRNA:** Guide RNA

524 **GWAS:** Genome-wide association study

525 **hnRNP-U:** Heterogeneous nuclear ribonucleoprotein U

526 **KCl:** Potassium chloride

527 **KO:** Knock-out

528 **LTD:** Long-term depression

529 **LTP:** Long-term potentiation

530 **LUHMES:** Lund human mesencephalic

531 **MSN:** Medium spiny neurons

532 **NHEJ**: Non-homologous end joining

533 **NMDAR:** N-methyl-D-aspartate receptor

534 **PBS:** Phosphate-buffered saline

535 **PLO:** Poly-L-Ornithine

536 **PSD:** Post-synaptic density

537 **PTZ:** Pentylenetetrazol

538 **ROS:** Reactive oxygen species

539 **SNP:** Single-nucleotide polymorphism

540 **TBS:** Tris-Buffered Saline

541 **TDP-43:** Transactivation response DNA-binding protein of 43kDa

542 **TH^+:** Tyrosine hydroxylase-positive

543 **TopoIIβ:** Topoisomerase IIβ

544 **TrkB:** Tropomyosin receptor kinase B

545 **Vps10p:** Vacuolar protein sorting (VPS) 10p

546 **VTA:** Ventral tegmental area

547 **WT:** Wild-type

548

549 **Acknowledgements**

550 We thank Dr Ian Adams for helpful discussions regarding scientific strategy and the manuscript
551 and Dr James Crichton for support with protocol optimisation and helpful comments on the
552 manuscript. KOG received salary support from an Alzheimer's Research UK award (ARUK-PPG2019B-
553 015) to KLE. TSJ is funded by the UK Dementia Research Institute which receives its funding from DRI
554 Ltd, funded by the UK Medical Research Council, Alzheimer's Society, and Alzheimer's Research UK,
555 and the European Research Council (ERC) under the European Union's Horizon 2020 research and
556 innovation programme (Grant agreement No. 681181).

557

558 **References**

559 **Adamec E, Vonsattel JP, Nixon RA (1999) DNA strand breaks in Alzheimer's disease. Brain Res**
560 **849:67–77. doi: 10.1016/s0006-8993(99)02004-1**

561 **Alemany S, Ribasés M, Vilor-Tejedor N, et al (2015) New suggestive genetic loci and biological**
562 **pathways for attention function in adult attention-deficit/hyperactivity disorder. Am J**
563 **Med Genet B, Neuropsychiatr Genet 168:459–470. doi: 10.1002/ajmg.b.32341**

564 **Crowe SL, Movsesyan VA, Jorgensen TJ, Kondratyev A (2006) Rapid phosphorylation of histone**
565 **H2A.X following ionotropic glutamate receptor activation. Eur J Neurosci 23:2351–2361.**
566 **doi: 10.1111/j.1460-9568.2006.04768.x**

567 **Davies G, Lam M, Harris SE, et al (2018) Study of 300,486 individuals identifies 148 independent**
568 **genetic loci influencing general cognitive function. Nat Commun 9:2098. doi:**
569 **10.1038/s41467-018-04362-x**

570 **Deinhardt K, Kim T, Spellman DS, et al (2011) Neuronal growth cone retraction relies on**
571 **proneurotrophin receptor signaling through Rac. Sci Signal 4:ra82. doi:**
572 **10.1126/scisignal.2002060**

573 **Duncan L, Yilmaz Z, Gaspar H, et al (2017) Significant Locus and Metabolic Genetic Correlations**
574 **Revealed in Genome-Wide Association Study of Anorexia Nervosa. Am J Psychiatry**
575 **174:850–858. doi: 10.1176/appi.ajp.2017.16121402**

576 **Fabbri C, Serretti A (2016) Genetics of long-term treatment outcome in bipolar disorder. Prog**
577 **Neuropsychopharmacol Biol Psychiatry 65:17–24. doi: 10.1016/j.pnpbp.2015.08.008**

578 Fabbri C, Tansey KE, Perlis RH, et al (2018) New insights into the pharmacogenomics of
579 antidepressant response from the GENDEP and STAR*D studies: rare variant analysis and
580 high-density imputation. Pharmacogenomics J 18:413–421. doi: 10.1038/tpj.2017.44

581 Fasci D, van Ingen H, Scheltema RA, Heck AJR (2018) Histone interaction landscapes visualized by
582 crosslinking mass spectrometry in intact cell nuclei. Mol Cell Proteomics 17:2018–2033.
583 doi: 10.1074/mcp.RA118.000924

584 Firsanov DV, Solovjeva LV, Svetlova MP (2011) H2AX phosphorylation at the sites of DNA double-
585 strand breaks in cultivated mammalian cells and tissues. Clin Epigenetics 2:283–297. doi:
586 10.1007/s13148-011-0044-4

587 Glerup S, Bolcho U, Mølgaard S, et al (2016) SorCS2 is required for BDNF-dependent plasticity in
588 the hippocampus. Mol Psychiatry 21:1740–1751. doi: 10.1038/mp.2016.108

589 Glerup S, Nykjaer A, Vaegter CB (2014a) Sortilins in neurotrophic factor signaling. Handb Exp
590 Pharmacol 220:165–189. doi: 10.1007/978-3-642-45106-5_7

591 Glerup S, Olsen D, Vaegter CB, et al (2014b) SorCS2 regulates dopaminergic wiring and is processed
592 into an apoptotic two-chain receptor in peripheral glia. Neuron 82:1074–1087. doi:
593 10.1016/j.neuron.2014.04.022

594 Greenwood TA, Lazzeroni LC, Maihofer AX, et al (2019) Genome-wide Association of
595 Endophenotypes for Schizophrenia From the Consortium on the Genetics of Schizophrenia
596 (COGS) Study. JAMA Psychiatry 76:1274–1284. doi: 10.1001/jamapsychiatry.2019.2850

597 Hegde ML, Banerjee S, Hegde PM, et al (2012) Enhancement of NEIL1 protein-initiated oxidized
598 DNA base excision repair by heterogeneous nuclear ribonucleoprotein U (hnRNP-U) via
599 direct interaction. J Biol Chem 287:34202–34211. doi: 10.1074/jbc.M112.384032

600 Hermey G (2009) The Vps10p-domain receptor family. Cell Mol Life Sci 66:2677–2689. doi:
601 10.1007/s00018-009-0043-1

602 Karlsson Linnér R, Biroli P, Kong E, et al (2019) Genome-wide association analyses of risk tolerance
603 and risky behaviors in over 1 million individuals identify hundreds of loci and shared
604 genetic influences. Nat Genet 51:245–257. doi: 10.1038/s41588-018-0309-3

605 Lotharius J, Barg S, Wiekop P, et al (2002) Effect of mutant alpha-synuclein on dopamine
606 homeostasis in a new human mesencephalic cell line. J Biol Chem 277:38884–38894. doi:
607 10.1074/jbc.M205518200

608 Ma Q, Yang J, Milner TA, et al (2017) SorCS2-mediated NR2A trafficking regulates motor deficits in
609 Huntington's disease. JCI Insight. doi: 10.1172/jci.insight.88995

610 Madabhushi R, Gao F, Pfenning AR, et al (2015) Activity-Induced DNA Breaks Govern the
611 Expression of Neuronal Early-Response Genes. Cell 161:1592–1605. doi:
612 10.1016/j.cell.2015.05.032

613 Madabhushi R, Pan L, Tsai L-H (2014) DNA damage and its links to neurodegeneration. Neuron
614 83:266–282. doi: 10.1016/j.neuron.2014.06.034

615 Malik AR, Szydlowska K, Nizinska K, et al (2019) SorCS2 Controls Functional Expression of Amino
616 Acid Transporter EAAT3 and Protects Neurons from Oxidative Stress and Epilepsy-Induced
617 Pathology. Cell Rep 26:2792–2804.e6. doi: 10.1016/j.celrep.2019.02.027

618 Miki Y, Mori F, Seino Y, et al (2018) Colocalization of Bunina bodies and TDP-43 inclusions in a case
619 of sporadic amyotrophic lateral sclerosis with Lewy body-like hyaline inclusions.
620 Neuropathology 38:521–528. doi: 10.1111/neup.12484

621 Mitra J, Guerrero EN, Hegde PM, et al (2019) Motor neuron disease-associated loss of nuclear TDP-
622 43 is linked to DNA double-strand break repair defects. Proc Natl Acad Sci USA 116:4696–
623 4705. doi: 10.1073/pnas.1818415116

624 Montecucco A, Zanetta F, Biamonti G (2015) Molecular mechanisms of etoposide. EXCLI J 14:95–
625 108. doi: 10.17179/excli2015-561

626 Morotomi-Yano K, Saito S, Adachi N, Yano K-I (2018) Dynamic behavior of DNA topoisomerase IIβ
627 in response to DNA double-strand breaks. Sci Rep 8:10344. doi: 10.1038/s41598-018-
628 28690-6

629 Mullaart E, Boerrigter ME, Ravid R, et al (1990) Increased levels of DNA breaks in cerebral cortex of
630 Alzheimer's disease patients. Neurobiol Aging 11:169–173. doi: 10.1016/0197-
631 4580(90)90542-8

632 Olsen D, Kaas M, Lundhede J, et al (2019) Reduced alcohol seeking and withdrawal symptoms in
633 mice lacking the BDNF receptor sorcs2. Front Pharmacol 10:499. doi:
634 10.3389/fphar.2019.00499

635 Olsen D, Wellner N, Kaas M, et al (2021) Altered dopaminergic firing pattern and novelty response
636 underlie ADHD-like behavior of SorCS2-deficient mice. Transl Psychiatry 11:74. doi:
637 10.1038/s41398-021-01199-9

638 Ortega-Martínez S (2015) Dexamethasone acts as a radiosensitizer in three astrocytoma cell lines
639 via oxidative stress. Redox Biol 5:388–397. doi: 10.1016/j.redox.2015.06.006

640 Rampersad SN (2012) Multiple applications of Alamar Blue as an indicator of metabolic function
641 and cellular health in cell viability bioassays. Sensors (Basel) 12:12347–12360. doi:
642 10.3390/s120912347

643 Scholz D, Pöltl D, Genewsky A, et al (2011) Rapid, complete and large-scale generation of post-
644 mitotic neurons from the human LUHMES cell line. J Neurochem 119:957–971. doi:
645 10.1111/j.1471-4159.2011.07255.x

646 Shanbhag NM, Evans MD, Mao W, et al (2019) Early neuronal accumulation of DNA double strand
647 breaks in Alzheimer's disease. Acta Neuropathol Commun 7:77. doi: 10.1186/s40478-019-
648 0723-5

649 Smith AH, Ovesen PL, Skeldal S, et al (2018) Risk locus identification ties alcohol withdrawal
650 symptoms to SORCS2. Alcohol Clin Exp Res 42:2337–2348. doi: 10.1111/acer.13890

651 Suberbielle E, Sanchez PE, Kravitz AV, et al (2013) Physiologic brain activity causes DNA double-
652 strand breaks in neurons, with exacerbation by amyloid-β. Nat Neurosci 16:613–621. doi:
653 10.1038/nn.3356

654 Thadathil N, Hori R, Xiao J, Khan MM (2019) DNA double-strand breaks: a potential therapeutic
655 target for neurodegenerative diseases. Chromosome Res 27:345–364. doi:
656 10.1007/s10577-019-09617-x

657 Tuxworth RI, Taylor MJ, Martin Anduaga A, et al (2019) Attenuating the DNA damage response to
658 double-strand breaks restores function in models of CNS neurodegeneration. Brain
659 Commun 1:fcz005. doi: 10.1093/braincomms/fcz005

660 **Wang H, Yang J, Schneider JA, et al (2020) Genome-wide interaction analysis of pathological**
661 **hallmarks in Alzheimer's disease. Neurobiol Aging 93:61–68. doi:**
662 **10.1016/j.neurobiolaging.2020.04.025**

663 **Yang J, Ma Q, Dincheva I, et al (2020) SorCS2 is required for social memory and trafficking of the**
664 **NMDA receptor. Mol Psychiatry. doi: 10.1038/s41380-020-0650-7**

665

666

667 **Figure Legends**

668 **Fig. 1** Exploration of a novel environment is associated with a transient increase in DSBs in the
669 dentate gyrus and the CA2. (a) Experimental design. Wild-type (WT) and *Sorcs2*$^{-/-}$ mice were divided
670 into three groups: 'home cage' (white), 'Novel E' (novel environment; light grey) and 'recovery' (dark
671 grey). For each brain region, the percentages of γH2A.X-positive nuclei was calculated in 5-6 month-
672 old WT (open bars) (b) and *Sorcs2*$^{-/-}$ mice (dotted bars) (c) belonging to one of the three
673 experimental groups. Three brain sections per region per mouse, n=3 per experimental group. (d)
674 Percentage of nuclei positive for γH2A.X in the DG of an independent set of wild-type (open bars)
675 and *Sorcs2*$^{-/-}$ (dotted bars) mice. Three brain sections per region per mouse, n=7-5. *$p<0.05$ (Mann-
676 Whitney test). Error bars represent median with interquartile range

677

678 **Fig. 2** Strategy for knocking out *SORCS2* in LUHMES using CRISPR/Cas9 genome editing. (a)
679 Experimental design of the CRISPR/Cas9 experiments. gRNA sequences (underlined) within *SORCS2*
680 exon 1 and exon 3 used (separately) to knock out the gene using CRISPR/Cas9 genome editing.
681 Created with BioRender.com. (b) Representative western blots show a complete loss of SORCS2 in
682 the knock-out (KO) clones after targeting exon 1 or exon 3. Samples loaded on the blot on the left
683 correspond to: 1 and 2 lysates obtained from wild-type (WT) LUHMES neurons (day 14), 3- 7- from
684 *SORCS2* KO exon 1 clones 1- 5 (day 14) generated by targeting exon 1. Samples loaded on the blot on
685 the right correspond to: 1 and 2 lysates obtained from WT LUHMES neurons (day 14), samples 3- 8-
686 from *SORCS2* KO exon 3 clones 1- 6 (day 14) generated by targeting exon 3. Sample 9 constitutes a

687 positive control (protein lysate from HEK293 cells overexpressing *SORCS2*). 'L' stands for ladder in
688 both blots. *SORCS2* exon 1 clone 4 and *SORCS2* exon 3 clone 5 did not survive neuronal
689 differentiation and were not included in any subsequent experiments.

690

691 **Fig. 3** Knocking out *SORCS2* leads to increased TopoIIβ-dependent DSB formation in LUHMES
692 neurons. (a) Representative confocal images from untreated (top row) and etoposide-treated
693 (bottom row) wild-type (WT) and *SORCS2* knock-out (KO) LUHMES neurons (day 14) immunostained
694 with γH2A.X (green) and 53BP1 (red), and counterstained with DAPI (blue). White arrows point
695 towards γH2A.X/53BP1 dual positive foci, and red- towards foci positive for γH2A.X only. Images
696 were taken at 100x magnification; scale bars: 10 µm. (b) Number of DSBs (γH2A.X/53BP1-positive
697 foci) per nucleus in untreated WT (white bar) and *SORCS2* KO (grey bar) LUHMES neurons (day 14);
698 n= 9 independent cell lines per genotype. Mann-Whitney test, $p > 0.05$. Error bars represent median
699 with interquartile range. (c) Number of DSBs (γH2A.X/53BP1-positive foci) per nucleus in etoposide-
700 treated (dotted bars) WT (white bars) and *SORCS2* KO (grey bars) LUHMES neurons (day 14); n=9
701 independent lines per genotype. * $p < 0.05$, Unpaired Student's t-test; error bars represent means ±
702 SD. (d) Number of DSBs (γH2A.X/53BP1-positive foci) per nucleus in etoposide-treated *SORCS2* KO
703 LUHMES neurons (day 14) generated by targeting exon 1 (n=4 independent cell lines) or exon 3 (n=5
704 independent cell lines). Mann-Whitney test, $p > 0.05$; error bars represent median with interquartile
705 range. Approximately 100 nuclei counted per cell line

706 **Fig. 4** Treatment with Glycine has no differential effect on DNA DSB formation in *SORCS2* knock-out
707 (KO) LUHMES neurons. No significant difference in the number of DSBs (γH2A.X/53BP1-positive foci)
708 per nucleus was identified between wild-type (WT) (white bar) and *SORCS2* KO (grey bar) LUHMES
709 neurons (day 14) following treatment with Glycine. Error bars represent means ± SD; n = 8
710 independent cell lines per genotype. Unpaired Student's t-test, $p > 0.05$

711

712 **Fig. 5** Knocking out *SORCS2* is associated with decreased neuronal viability at late (day 14), but not
713 early (day 6) stages of neuronal differentiation. Neuronal viability of wild-type (WT) (white bar) and
714 *SORCS2* knock-out (KO) (grey bar) LUHMES neurons measured at early (day 6) (a) and late (day 14)
715 (b) stages of differentiation. ** $p < 0.01$ (unpaired Student's t-test); Error bars represent means ± SD;
716 n = 8-9 independent cell lines per genotype

717

718

719

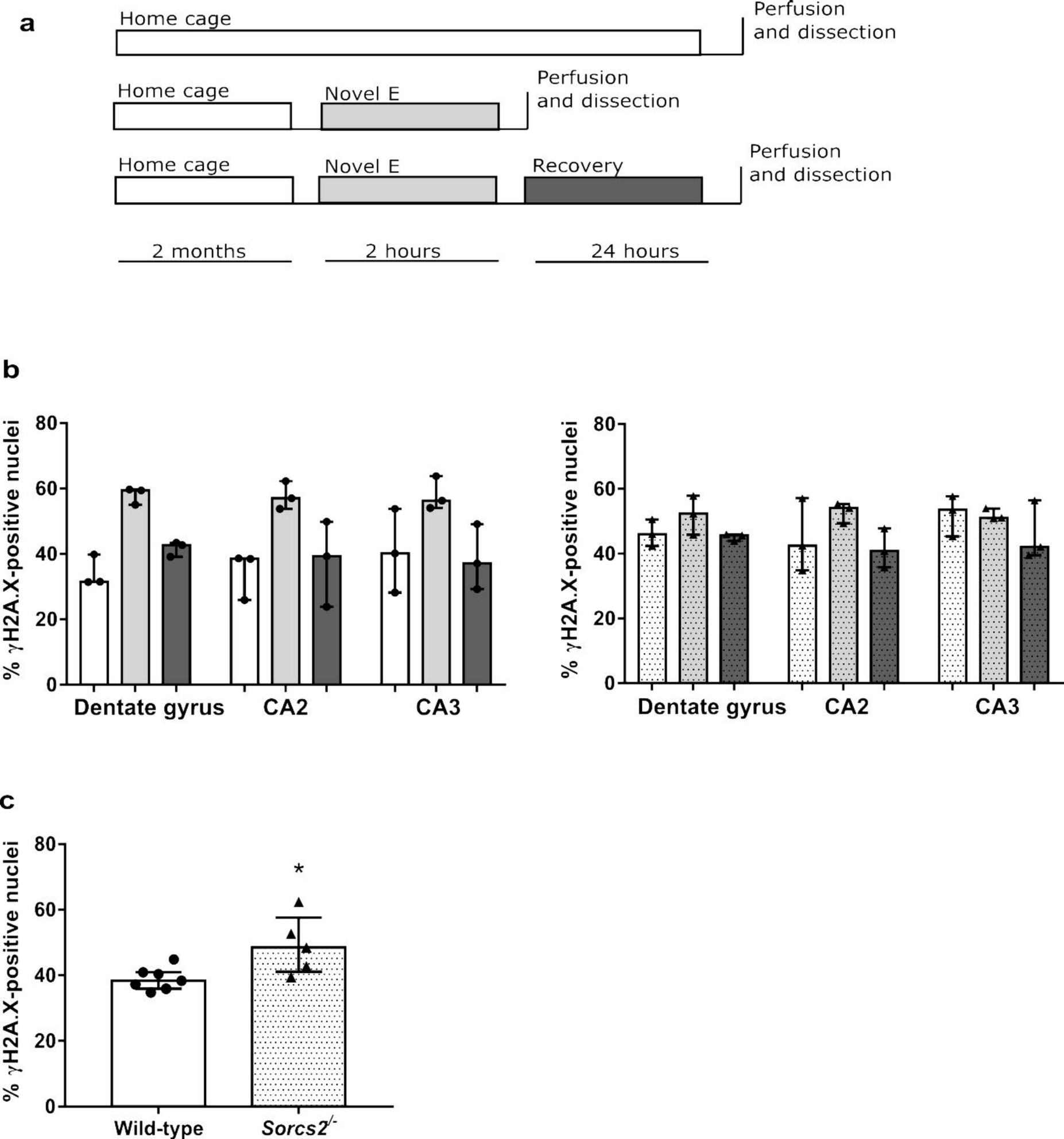
a
Home cage
Perfusion and dissection
Home cage
Novel E
Perfusion and dissection
Home cage
Novel E
Recovery
Perfusion and dissection
2 months
2 hours
24 hours
b
% γH2A.X-positive nuclei
80
60
40
20
0
Dentate gyrus
CA2
CA3
% γH2A.X-positive nuclei
80
60
40
20
0
Dentate gyrus
CA2
CA3
c
% γH2A.X-positive nuclei
80
60
40
20
0
*
Wild-type
Sorcs2-/-

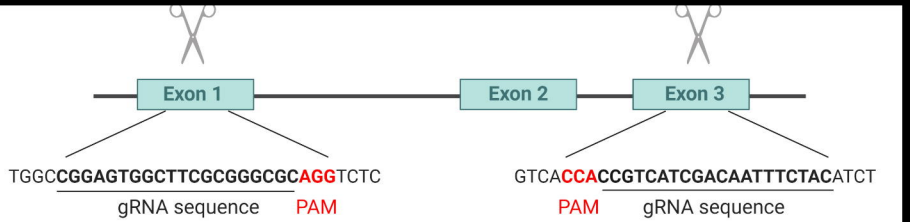
Exon 1
Exon 2
Exon 3
TGGCCGGAGTGGCTTCGCGGGCGCAGGTCTC
gRNA sequence
PAM
GTCACCACCGTCATCGACAATTTCTACATCT
PAM
gRNA sequence

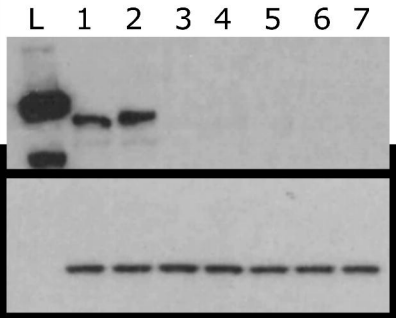
L 1 2 3 4 5 6 7

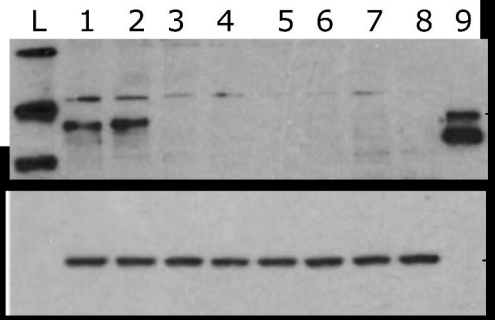
L 1 2 3 4 5 6 7 8 9

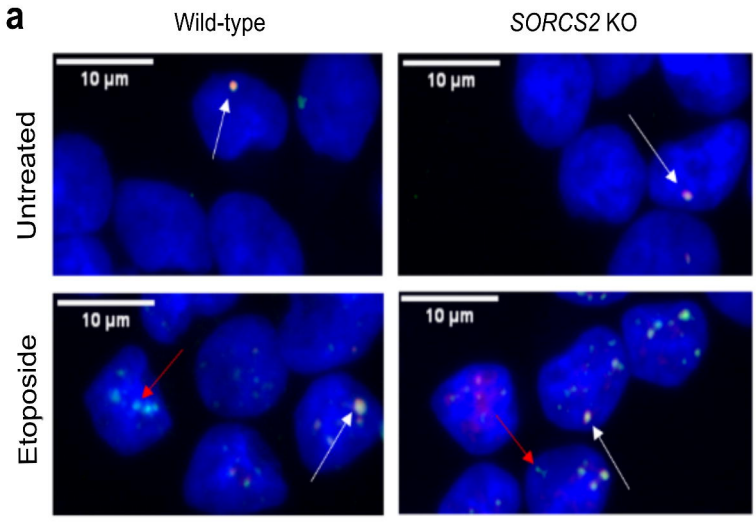
a
Wild-type
SORCS2 KO
Untreated
Etoposide
10 µm
10 µm
10 µm
10 µm

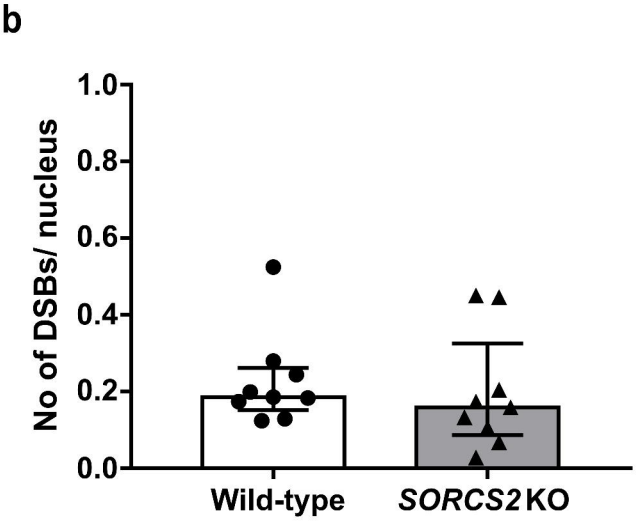
b
No of DSBs/ nucleus
1.0
0.8
0.6
0.4
0.2
0.0
Wild-type
SORCS2 KO

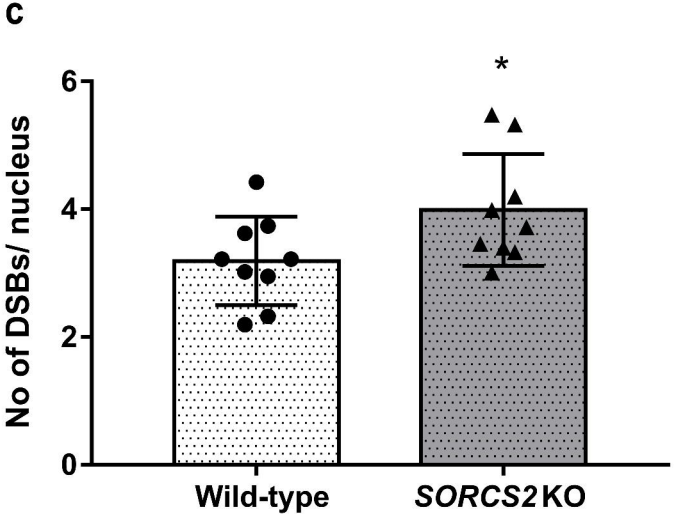
c
No of DSBs/ nucleus
6
4
2
0
*
Wild-type
SORCS2 KO

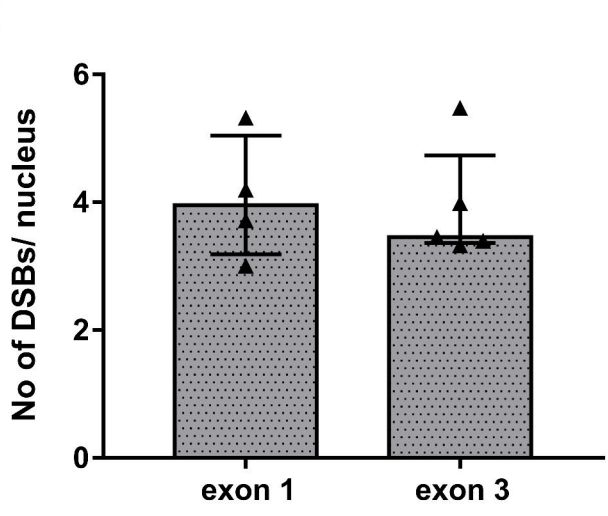
d
No of DSBs/ nucleus
6
4
2
0
exon 1
exon 3

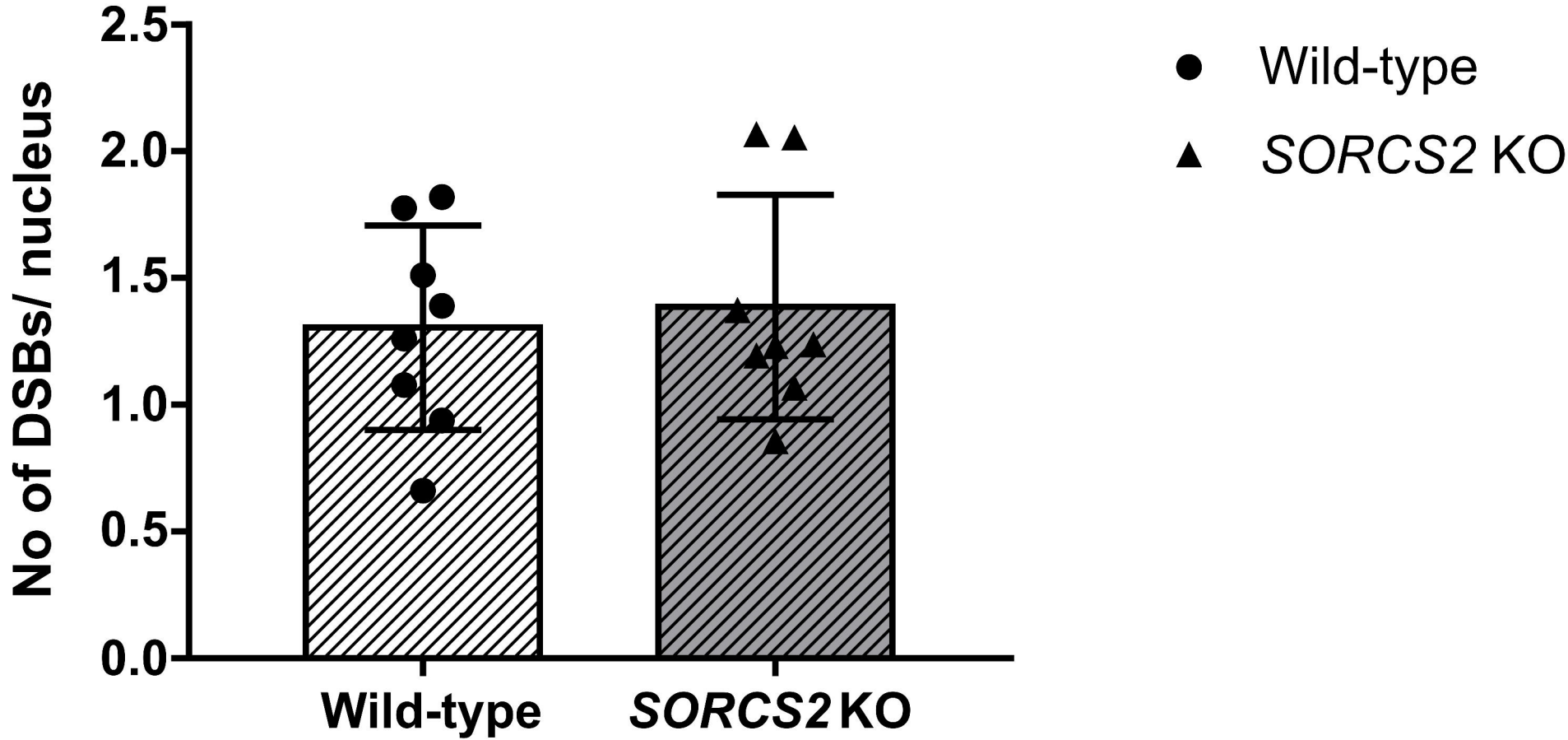
No of DSBs/ nucleus
2.5
2.0
1.5
1.0
0.5
0.0
Wild-type
SORCS2 KO
Wild-type
SORCS2 KO

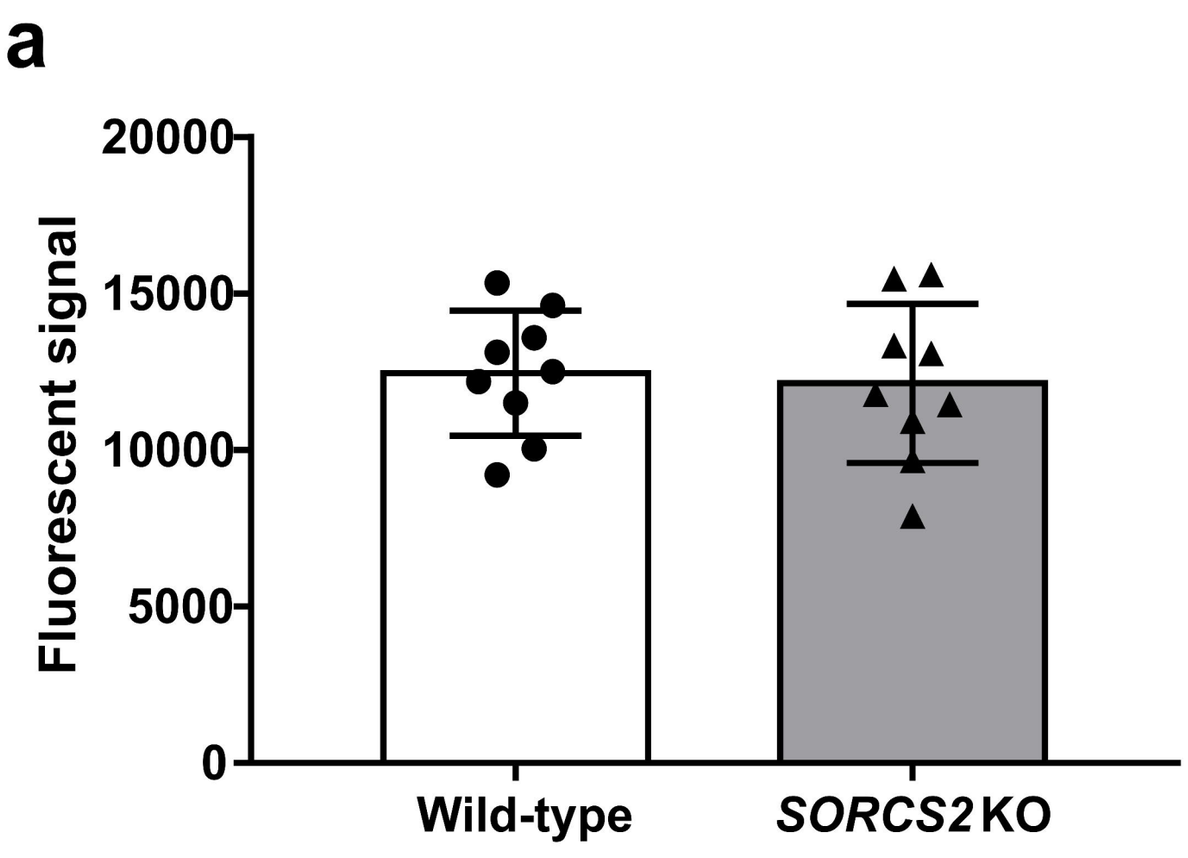
a
20000
15000
10000
5000
0
Fluorescent signal
Wild-type
SORCS2 KO

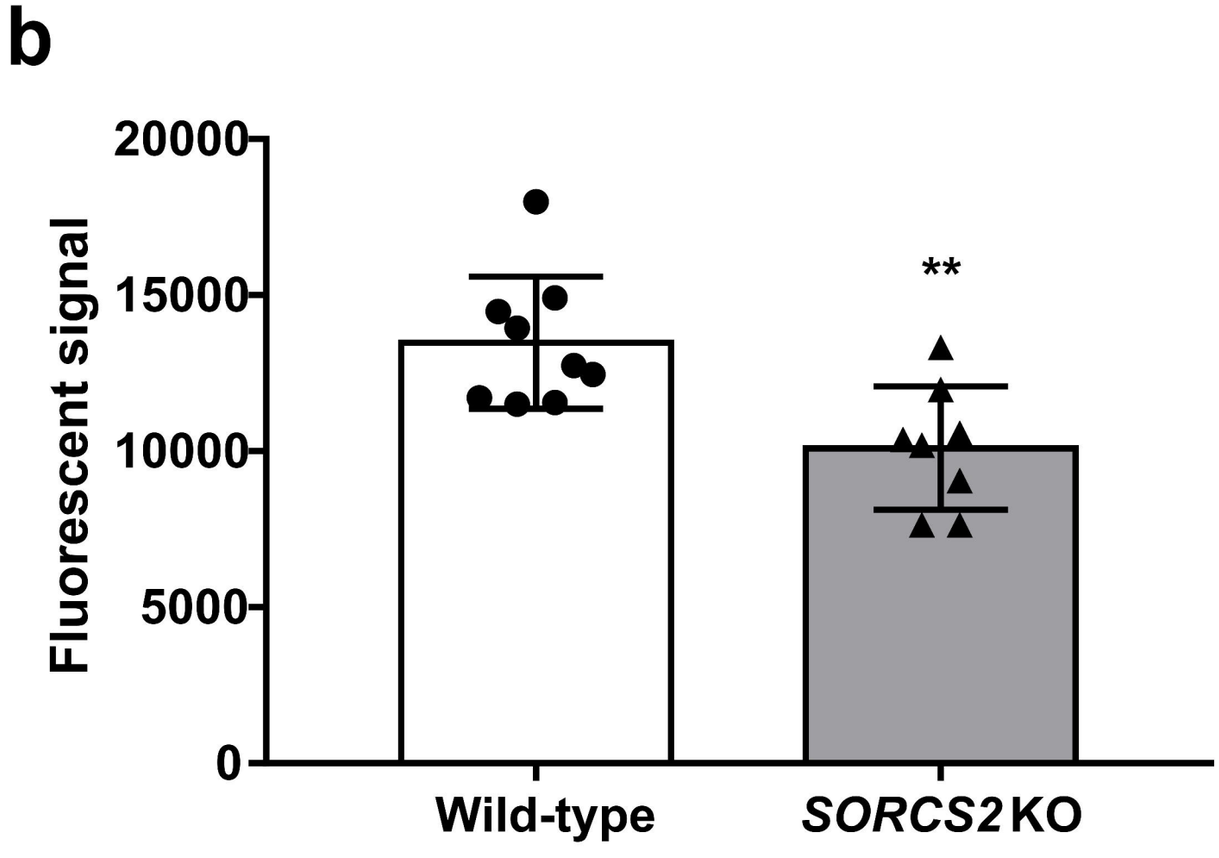
b
20000
15000
10000
5000
0
Fluorescent signal
**
Wild-type
SORCS2 KO